

Critical behavior in cloud formation

Brian D. Busemeyer

(Dated: May 8, 2017)

The connection between environmental changes and cloud formations remains an important, but poorly understood, component of climate research. Much of the difficulty in describing cloud formation lies in the multi-scale character of the underlying features of cloud formation. Recently, both observations of cloud formation via satellite and detailed simulations of cloud dynamics have suggested the transition between clear and cloudy skies carries signatures of a phase transition. These signatures include universal power law scaling, connections to predator-prey dynamics, and singularities in the response to external perturbations. I explore three investigations into these discoveries and discuss the implications of their assumptions and their results.

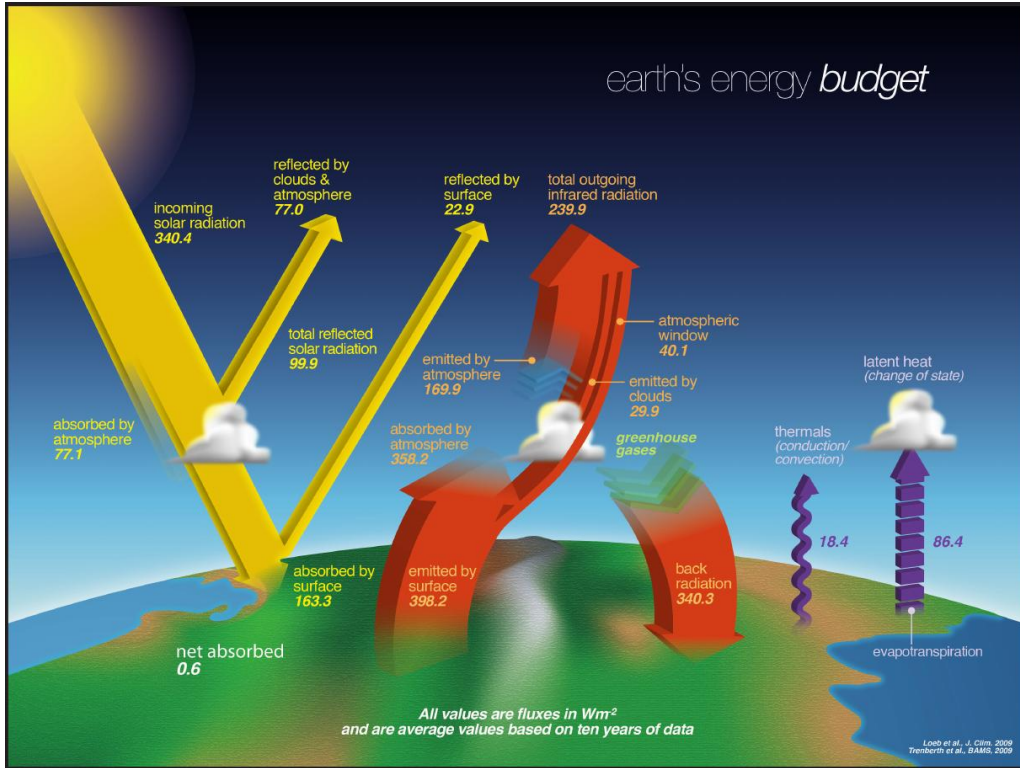


FIG. 1: Breakdown of the energy budget of sunlight incident on Earth's surface. Part of the sunlight is reflected by the clouds and atmosphere, while much of the remaining warms Earth's surface. Part of this energy then vaporizes water and induces convection, producing more cloud cover. This complex relationship is part of what makes climate predictions difficult. Reproduced from ref. [3].

I. INTRODUCTION

A lack of understanding of the conditions giving rise to widespread cloud formation remains a significant obstacle in the study of Earth's climate. The accurate prediction of the formation of clouds is critical for accurate predictions of climate change lies fundamentally due to Earth's interaction with the sun. When exposed to solar radiation, an object floating in space will absorb a certain percentage of the incoming light as heat. As the object warms, the temperature will rise until the energy flux of the black body radiation matches the incoming radiation. The greater the fraction of radiation is absorbed by the object, the higher the temperature must be in order to balance the energy flux into the system and keep the system in equilibrium. The same logic applies to the Earth, but in a more sophisticated way. Light incident on Earth's atmosphere is partially reflected by clouds in the atmosphere, as well as objects on the surface. Likewise, the black body radiation of the Earth is partially absorbed by molecules in the atmosphere and partially radiated back to Earth, otherwise known as the "greenhouse effect." Some of the incident energy also vaporizes water, becoming the latent heat of the formation of water vapor which may go on to form clouds. Some energy also powers convection cycles, which may further affect cloud formation. The details of this process are carefully studied [1, 2] and illustrated in Fig. 1.

Although the effects of clouds on the energy budget represent an important component,

it remains difficult to predict processes of cloud formation. Uncertainty in the sensitivity of cloud formation to environmental changes is currently the largest source of error in climate modeling. One numerical study conducted 15 model climate calculations that attempt to predict annual climate change, and found that the predictions for cloud response to climate change both had the largest variations between models, as well as the largest deviations from observed changes on Earth [4]. Accurate simulations of climate change depend on improvements to our understanding of cloud formation.

The difficulty in modeling cloud formation arises from its multi-scale character. Features on the order of 10s of meters are important for accurate simulations, although interesting features may exist on length scales of 1000s of meters [5]. Parametrizing and coarse graining these features may be difficult as well. For example, it is difficult to generate deterministic models for cloud formation that can reproduce spacial variations in cloud formations. Stochastic techniques must be used instead, in order to capture uncertainties in behavior below the length scales simulated in experiment [6]. Additionally, the large scale of atmospheric effects means no controlled, laboratory-based experiments are possible. Researchers must gather information from a combination of uncontrolled observations of Earth's atmosphere and detailed, but computationally expensive, simulations based on fundamental physics such as the Navier-Stokes equations.

The multi-scale character of the cloud formation has motivated some researchers to explore the possibility of applying statistical mechanics to understanding the large-scale behavior of clouds. Although work in this field has not yet been made rigorous, some simulations and observations suggest that ideas of critical phenomena may be relevant to cloud formation. Note this critical behavior is distinct from the well-established first-order transition that occurs when clouds condense into precipitation. Instead, this transition refers to the larger-scale transition that occurs when clouds coalesce or precipitate over 100s to 1000s of kilometers. Observations and calculations have found emergent behavior that is suggestive of behavior that is described in statistical mechanics. In particular, moist air tends to sensitive to properties in the atmosphere that cause it to spontaneously form clouds, and this transition displays behavior reminiscent of universality [7]. Clouds also can form periodic patterns reminiscent of antiferromagnetic order, related to processes turning converting clouds to rain and back again [5, 8]. The purpose of this paper is to explore some of these observations and discuss how the process of cloud formation can be connected to phase transitions. It will also explore how these observations may help in our understanding of cloud formation in the context of climate modelling.

II. OBSERVATIONS FROM SATELLITE DATA

Peters and Neelin released a study in 2006 finding that satellite images of tropical rainfall rates exhibited evidence of a phenomenon known as “self-organized criticality,” and that rainfall rates displayed features that can be described as universal critical exponents [7]. They utilized data available from the Tropical Rainfall Measuring Mission from 2000 to 2005, which utilized microwaves to measure rainfall rate, P , and water vapor, w , cloud liquid water and sea surface temperature. From these observables, they compute $\langle P \rangle(w)$, defined to be the average P at fixed w over all regions and times over the course of the mission. The authors found some features of critical transition in these variables.

To motivate studying the critical behavior of this system, Peters and Neelin investigate the so-called quasi-equilibrium postulate. In some systems, the order parameter of the

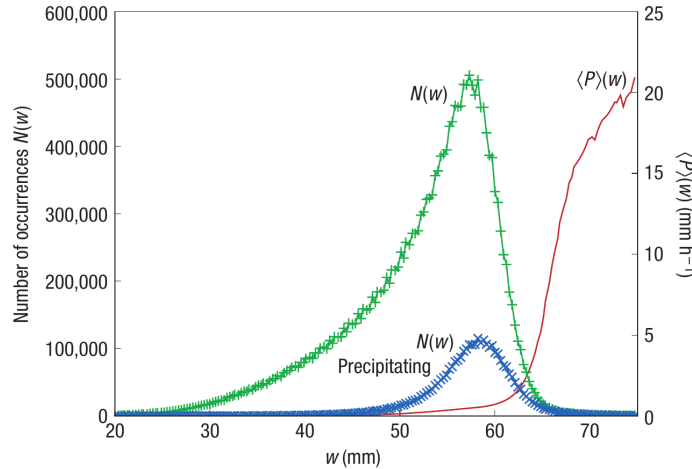


FIG. 2: (Green +) Number of times water vapor, w , was observed over 5 years of satellite data in the tropics. (Blue \times) same as previous, but only those that were classified as precipitating. (Red line only) Average precipitation for satellite pixels with that amount of water vapor w . This demonstrates that the system generally oscillates about the transition point, defined as the point of water vapor saturation where precipitation tends to occur. Below the peak, evaporation and convection increase the water vapor until it becomes saturated, then over-saturated. Above the peak, precipitation is triggered, and the air quickly dissipates the excess moisture through rain. Reproduced from ref. [7].

system may be coupled to an external driving force such that the system is driven toward its critical transition whenever it exists in a stable phase. Such systems the system will be perpetually be near their critical points [7]. The postulate is that the cloud to precipitation system is such a system [9]. When the air is sub-saturated with water, heat evaporates water and increases the saturation. The warm, moist air rises and condenses into clouds. When the clouds become over-saturated, a small event triggers precipitation, which quickly dissipates the water vapor from the air into liquid water. To confirm this behavior, the authors histogram the number of times a pixel from the satellite image was at a given w , and compare it to the average precipitation $\langle P \rangle(w)$, reproduced in Fig. 2. The results demonstrate that the majority of the time, the atmosphere in the tropics is quite close to the transition to precipitation, consistent with the notion that the state of the system is attracted to the transition. Thus also implies that the majority of observations of cloud behavior will be near this transition, and therefore critical phenomena will be relevant.

To investigate whether this transition exhibits critical phenomena, the authors attempt to fit an asymptotic function of the form

$$\langle P \rangle(w) = a(w - w_c)^\beta$$

near the critical transition. Here, w_c represents the region-dependent critical vapor density before precipitation, and a represents a region-dependent constant. The region-dependence enters because different regions' temperatures and geological features can impact w_c and the magnitude of the precipitation that is triggered. The process of scaling away these differences is shown in Fig. 3. By adjusting the plots in a simple, consistent way, the functional dependence of $\langle P \rangle(w)$ shows good data collapse, particularly near and above the w_c transition into precipitation.

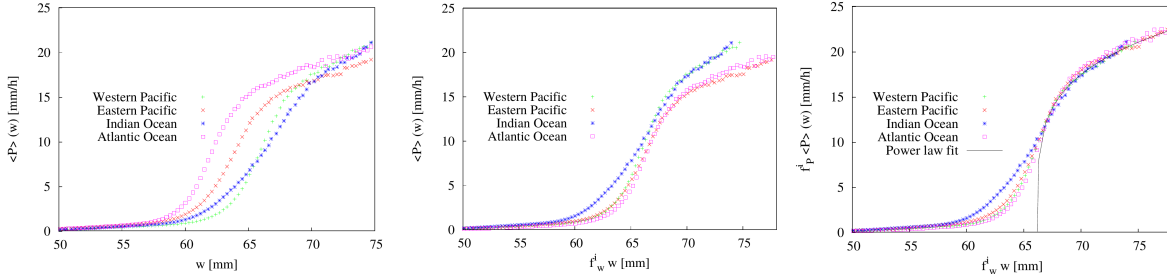


FIG. 3: Process of scaling $\langle P \rangle(w)$, the average rainfall as a function of w , vapor density. **Left:** unscaled, raw data. Data shows similar trends, but there are quantitative differences. **Middle:** w multiplied by a region-dependent factor (f_w^i) that sets their transition vapor density the same. **Right:** scaling $\langle P \rangle(w)$ by a region-dependent value (f_P^i) to set the precipitation values approximately the same. After this scaling process, the functional form of $\langle P \rangle(w)$ is similar for all regions near the critical transition. A power law fit is shown as a solid line. Reproduced from ref. [7].

They also define a susceptibility by $\chi(w, L) = L^d \sigma_P^2(w, L)$, where σ_P^2 is the variance of the distribution of P across regions and times, L represents the spacial resolution of the data, and d represents the dimensionality. In their case, they integrate over the height of the atmosphere (w is the water density per area), therefore $d = 2$. The value of $\sigma_P(w, L)$ along side $\langle P \rangle(w)$ is shown in Fig. 4. Consistent with what might be expected from critical behavior, this definition of $\chi(w, L)$ diverges near the transition point. The resulting power law fit finds that the same critical exponent $\beta \approx 0.215$ fits all the different regions, varying between regions by only ± 0.02 .

To calculate other critical exponents and verify that the data collapse is indeed due to a critical transition (rather than something like theorem of corresponding states), the authors perform what they call a “finite size” analysis (although I have issues with this, explained in the conclusion). Since they cannot vary the system size, they instead vary the spacial resolution by averaging over blocks of the satellite data. They use what they call the finite size scaling ansatz $\chi(w, L) = L^{\gamma/\nu} \tilde{\chi}(\Delta w L^{1/\nu})$. Here, γ and ν are defined analogously to other transitions, and $\tilde{\chi}$ is a scaling function. The results of the analysis are presented in Fig. 4 (right) and find that $\gamma/\nu \approx 1.54(4)$. The specifics of how this fitting is performed is explained in the figure caption. The data collapse near the critical transition is again suggestive that critical exponents associated with a phase transition are being observed in the satellite data.

III. MODELS FOR BEHAVIOR

Based on observations of cloud formation similar to Peters and Neelin (reported above), some work has been done to provide coarse-grained models the reproduce the phase transition from cloudy to clear atmospheres. If the transition is indeed representative of a critical point, coarse grained models may be a good representation of large-scale behavior because shorter scale behaviors are correlated. This intuition motivates the investigation of simplified models that attempt to reproduce qualitative long-range behaviors, two of which are presented here.

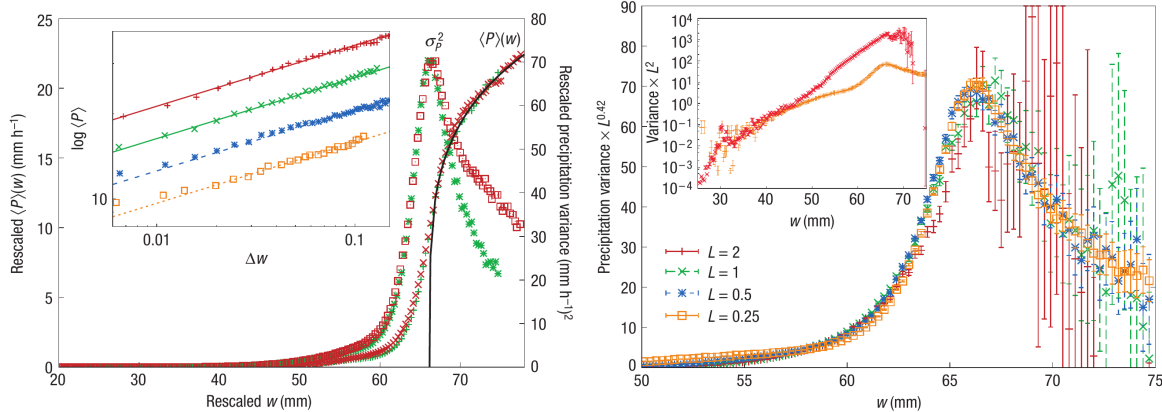


FIG. 4: **Left:** a plot of the scaled order parameters $\langle P \rangle(w)$ for two regions (western and eastern Pacific), along with the power law fit. On a parallel axis, the variance in the order parameter (among the regions and times considered) is shown, showing a sudden increase reminiscent of the singularity in the fluctuations near a critical transition. The inset displays the log-log plot of the power law fit for the all the regions, offset by a constant for easy of plotting. **Right:** “finite size” scaling analysis of the transition. Due to noise in w and w_p the authors determine the exponents in $\chi(w, L) = L^{\gamma/\nu} \tilde{\chi}(\Delta w L^{1/\nu})$ by noting that $\sigma_P^2 \propto L^{\gamma/\nu - d}$ (where $d=2$) and finding the γ/ν that products the data collapse near the peak. The inset shows that farther from the w values near the peak, the data agrees between regions when $\gamma/\nu = 0$, suggesting the collapse near the transition is indeed from critical phenomena. Reproduced from ref. [7].

A. Predator-Prey model for clouds and precipitation

The observations of critical-like behavior in cloud formation, together with the observation that the system tends to be driven towards its critical point, suggests that it may be possible to devise simplified models that coarse-grain the complicated small-scale degrees of freedom, yet still capture some of the emergent behavior. Fine-scale (10s of meters) simulations of the Navier-Stokes equations found that although the cloud formation and precipitation responses to small perturbations of the environment were complex, the systems tended to prefer distinct modes of behavior [10]. This emergent simplified behavior suggests that simplified models may provide an alternative means to reproduce the same results.

Motivated by these detailed simulations, Koren and Feingold attempted to explain some of the dynamics of cloud-precipitation transitions using a simplified predator-prey model [5]. The relationship between predators and prey can be modeled by the Lotka-Volterra equations. These equations make prey growth proportional to prey population and prey death proportional to predator population. Predator population is proportional to both predator and prey populations. This produces a cyclic behavior of populations shown in Fig. 5(left). Of course, many simplifying assumptions have been made in this model. For example, spatial variations of the populations are completely neglected, and external factors such as food supply for prey and perhaps disease and other harsh conditions are neglected. Nonetheless, this model has reproduced some qualitative behaviors in a variety of systems [5, 11, 12], suggesting detail such as disease are not important to capture the qualitative behavior of the system. This oscillatory behavior is partially reproduced in the detailed Navier-Stokes

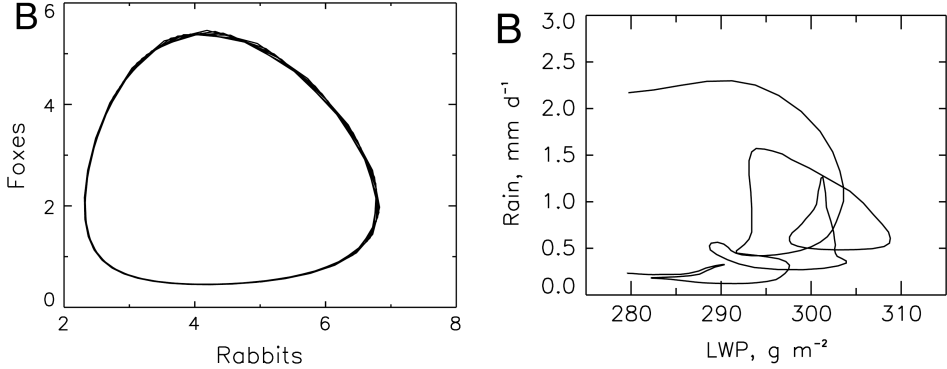


FIG. 5: **Left:** population cycle for predator and prey populations for foxes and rabbits (respectively). The populations undergo cycles associated with growth of prey, then growth of predators, then overpredation and the decline of prey population, then decline of predator population due to starvation. In this simplified model, the populations are completely cyclical, so as time progresses the curve follows the same path many times in circles. Populations of the animals are completely periodic, and phase-shifted with respect to each other. **Right:** for comparison, the linear water path (LWP), essentially a measure of cloud height, vs. the rainfall rate, generated by detailed simulations of the Navier-Stokes equations [10]. In these simulations, the quantities rise and fall in phase-shifted manner; however, they are not completely periodic, and slowly approach a stable fixed point. Reproduced from ref. [5].

simulations, as shown in Fig. 5(right).

Based on this similar behavior, and observing that rain tends to “consume” clouds much like predators consume prey, Koren and Feingold attempt to use simple approximations to derive a cloud-precipitation model that resembles a predator-prey model like the Lotka-Volterra equations. Much like the predator-prey model, the authors’ model neglects spacial variations in clouds and precipitation. Instead the amount of clouds is represented by a single variable, H , representing cloud depth, whose growth rate is determined by

$$\frac{dH}{dt} = \frac{H_0 - H}{\tau_1} + \dot{H}_r(t - T)$$

Here, H_0 represents the cloud depth the environment drives towards, τ_1 represents the time constant associated with cloud growth, and T represents the delay from processes that begin precipitation. $\dot{H}_r < 0$ represents the loss in clouds due to rain. The authors note that the presence of aerosol, or small particles that act as nucleation sites for cloud particles, can decrease the tendency of cloud particles to form rain and also affect albedo in climate models. Thus the authors include it as a separate variable in their simulations. Using results from the literature, they connect \dot{H}_r to the cloud height, H , and density of aerosol, N_d : $\dot{H}_r(t) = -\alpha H(t)^2 / c_1 N_d$. Here, α and c_1 are constants that depend on temperature and details of the clouds, which are neglected in the dynamics. A similar procedure for droplet formation produces the equation

$$\frac{dN_d}{dt} = \frac{N_0 - N_d}{\tau_2} - c_2 N_d(t - T) R(t); \quad R(t) = \frac{\alpha H^3(t - T')}{N_d(t - T')}$$

τ_2 , T' are analogous definitions for the process of removing aerosols from the air via precipitation. $R(t)$ is the rainfall rate in this context. This produces a coupled set of differential

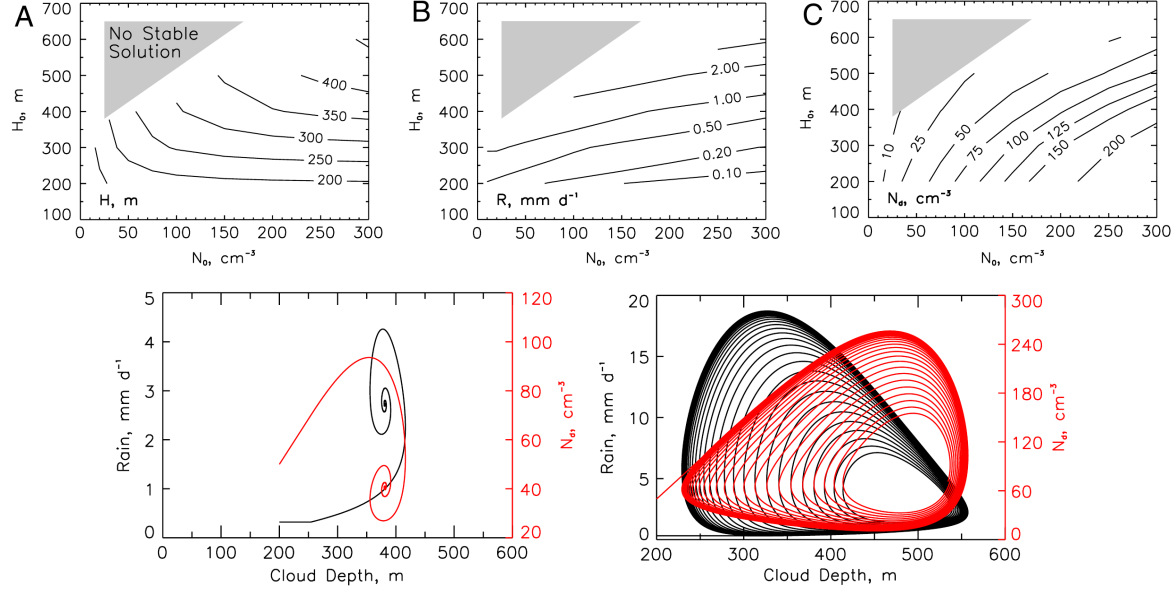


FIG. 6: Finite difference results for simplified predator-prey model for cloud formations. **Top:** Contour plots of the stationary state values of H (cloud depth), R (rain rate), and N_d (density of aerosol) as a function of H_0 and N_0 (the cloud depth and aerosol concentration that the system converges towards based on details in the environment). H generally increases with either H_0 or N_d consistent with the fact the both parameters increase the amount of moisture trapped in the particles that make up clouds. Large concentrations of moisture with small concentrations of aerosol result in large precipitation rates, which generally results in dynamics which do not settle into a stationary state, represented as the grey regions. The aerosol concentration decreases with increasing precipitation, and consequently decreases near the precipitating region. The shift in (A) from strong dependence on N_d to weak represents a mode switch from rainy, unstable cloud formation to stable cloud formation. **Bottom:** Dynamics of cloud depth, rain rate, and aerosol concentration for low (left) and high (right) rainfall. Low rainfall occurs for low H_0 and high N_0 , while high rainfall occurs for the opposite. The high rainfall mimics the behavior of the simple Lotka-Volterra equations of Fig. 5(left), while the low rainfall mimics the damping oscillations found from the detailed simulations of Fig. 5(right). Thus this model can span the behavior between the two systems, and thus connects the predator-prey model behavior to the behavior of the detailed cloud dynamics. Reproduced from [5].

equations for clouds, aerosol, and precipitation analogous to the simpler Lotka-Volterra equations.

Using a finite-difference approximation to the solutions, Koren and Feingold then present numerical solutions to the differential equations, and find qualitative similarities to the more detailed Navier-Stokes equations. For some sets of parameters the simulations approach a stationary state, and the properties of these stationary states are explained in Fig. 6. Importantly, the system predicts two primary regimes associated with the presence of aerosols. For high aerosol concentration, droplet formation is suppressed, and the population oscillations converge quickly to a steady state, where clouds are stable at a fixed cloud depth. For low aerosol concentration, the clouds are vulnerable to precipitation and experience extended periods of reduced cloud depth. This corroborates evidence in both the numerical simula-

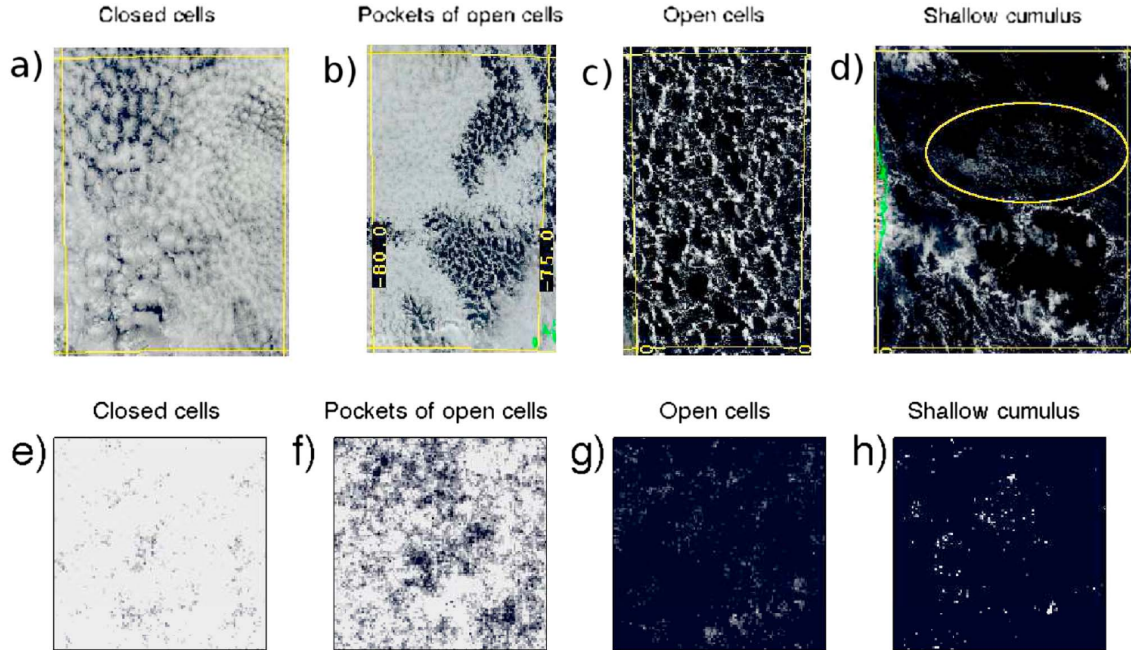


FIG. 7: **Top:** Satellite images of cloud formations showing the “open” and “closed” cell phases of cloud formation in the atmosphere. The “shallow cumulus” diagram notes that not all cloud formations are readily categorized by these phases. **Bottom:** Solutions corresponding to these phases from the stochastic diffusion model outlined in the text. Reproduced from [8].

tions, and the behavior of clouds in nature, which tend to either form stable “closed cell” formations or clearer “open cell” formations. Examples of the distinct behavior of these two phases are shown in Fig. 7(top).

B. Stochastic model and similarities to Ising model

A more recent study by Stechmann and Hottovy attempted to explain the shift between these “open” and “closed” cell states in terms of a highly simplified stochastic diffusion process [8]. Satellite view of cloud phases depict a variety of formations that seem to form condensed phases varying between open to closed cells much as an Ising model varies from spin up to spin down as the H -field moves from a positive to negative value. An example of this shift is shown in Fig. 7. Their model attempts to incorporate the spacial variation in the directions tangent to earth’s surface, considering the height-integrated quantity $q(x, y, t)$ representing the total total water in a column of atmosphere in the boundary layer at (x, y) . The $q(x, y, t)$ is shifted so that $q = 0$ when the column of air is at its saturation point. The model they consider takes the form

$$\partial_t q = b \nabla^2 q - \frac{1}{\tau} q + D \dot{W} + F$$

The model idealizes the movement of water in the atmosphere as represented by stochastic diffusion. The first term, $b \nabla^2 q$, represents the diffusion of water as a result of many eddy currents that are below the scale the model considers. The next two terms represent highly

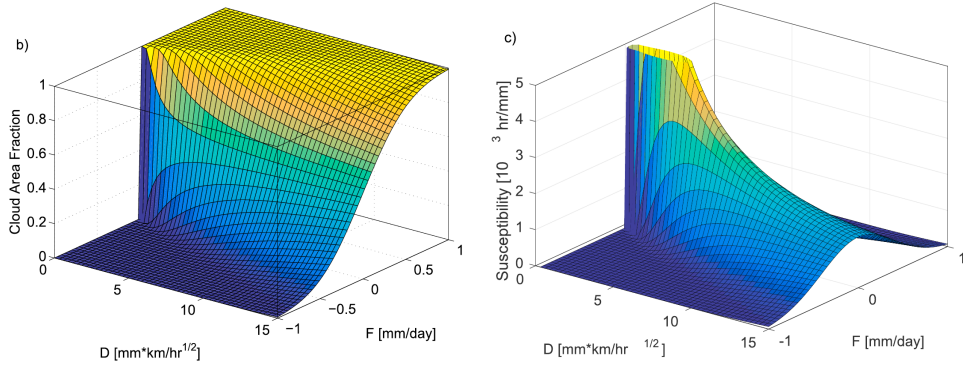


FIG. 8: **Left:** Analytic solution for the mean cloud area fraction according to the stochastic diffusion model. This diagram holds b and τ fixed and varies D and F much like how H and T would be varied in the Ising model. **Right:** The susceptibility, defined as $\partial\bar{\sigma}/\partial F$ measure the sensitivity of the phase to changes in the environment. Reproduced from [8].

simplified models for turbulence, $-q/\tau$ representing additional diffusion that results, and \dot{W} being spatially and temporally random noise. Finally F represents a source sink term (depending on the sign). The values of the parameters, b , τ , D , and F are dependent on the cloud environment, and for the purpose of this study, they fix b and τ and focus on D and F due to their connections to environmental effects of interest. In particular, temperature sea surface temperature has a direct effect on both D and F . Higher sea temperatures will produce more atmospheric water vapor as well as increased noise due to turbulence, as depicted by the purple arrows in Fig. 1. The other two parameters, b and τ are set by the scales of variations in space and time, and are fitted to observational data.

In the interest of interpreting the cloud formation as a phase transition, the authors consider a cloud indicator variable:

$$\sigma(x, y, t) = \begin{cases} 1 & \text{if } q(x, y, t) > 0 \\ 0 & \text{if } q(x, y, t) < 0 \end{cases}$$

The benefit of the simplified model is that the mean cloud indicator value are analytically soluble. Because the model is stochastic, the stationary state solution to the equation is also stochastic in nature. The analytic solution of the equation can be used to calculate $\bar{\sigma}$, the mean cloud indicator, as well as the effect of environmental factors on $\bar{\sigma}$. The solutions are illustrated in Fig. 8 and samples from the solutions appear in the bottom row of Fig. 7.

Interestingly, the solutions to the stochastic diffusion model are reminiscent of an Ising model in 1-d. In fact, the parameters of the diffusion model outlined above have a simple interpretation in terms of the Ising model parameters.

- b represents J , the interaction term between spins.
- D represents the randomizing effect of turbulence, and is analogous to temperature in the Ising model.
- F represents H , in that it is an external effect that biases the system to either clear or cloudy sky.

The τ parameter, however, does not have any analogy with the Ising model. This suggests the singularity occurring at $D = 0$ (zero turbulence) represents the first order transition

analogous to the zero-temperature transition in the 1-*d* Ising model as H changes sign. At the zero turbulence limit, the solution space catagorizes the phases of cloud formations in terms of two phases, open and closed, which correspond to clear and cloudy conditions. Introducing a small amount of turbulence function much like temperature, causing random coexistence of open and closed phases.

IV. SUMMARY AND CONCLUSIONS

The three results explored in depth here all explore aspects of cloud dynamics that suggests concepts of critical behavior may be applicable to cloud formations. The satellite imagery and scaling analysis suggested that the cycle between cloud formation and dissipation through precipitation may be critical point. Moreover the critical behavior is quite important because this system is constantly being driven through the transition by external factors that push the air towards saturation and precipitation. Data collapse near the transition between saturation and precipitation was suggestive that power-law scaling and universal scaling exponents may exist for this transition. The fact that detailed simulations of the Navier-Stokes equations can also be qualitatively reproduced through simple effective models is also suggestive of critical behavior. Effective coarse-graining techniques rely on long correlation lengths associated with the phase transition. These coarse-grained models also are more numerically soluble for large-scale and long-time simulations, and hence may be useful for gaining insight into how climate change may impact cloud formation, which in turn affects the course of climate change. The diffusion model replicates the results of the satellite scaling analysis, finding that transitions between cloudy and clear skies can be connected to singular behavior in a response function. The resulting solution for the order parameter, cloud fraction, is highly reminiscent of the behavior of the 1-*d* Ising model, which exhibits a critical point at zero temperature.

Although these results are certainly interesting and suggestive, the concrete connection to phase transitions is not yet clear. Although all three of these results suggest phase transitions, they each make several simplifying approximations that may be unjustified, and only make qualitative connections to critical behavior. The satellite data does indeed show data collapse; however, the finite size scaling does not quite seem convincing that the collapse is due to critical behavior. Finite size scaling utilizes the changes in the behavior of the system as the size of the system, measured by lengthscale L (e.g. a square or box of side L) changes compared to the correlation length, ξ . They affectively change L by averaging over pixels in the satellite data, but this also coarse-grains the data, reducing ξ simultaneously. Thus, it is not clear to me this is a proper way to conduct finite size scaling. The analysis in terms of the predator-prey model completely ignores variations in space and time, and does not draw any well-defined connection between the results and the open and closed phases seen in satellite images. The diffusion equation does see a sharp critical transition, but only in the limit of zero turbulence, and completely neglects spacial and temporal dependence in the parameters. In reality the is always turbulence in weather patterns, and this turbulence is likely more significant when considering spacial variations like mountains and other geological features, as well as temporal variations like temperature variations between day and night as well as seasonal variations. Nonetheless, given that these three fairly disparate approaches all reach somewhat similar results seems encouraging that some truth may be apparent in them. Given improvements to the simulations, such as incorporating the spacial or temporal dependence in the parameters, potentially the applicability of their results may

be better established. If indeed the machinery of critical phenomena applies to cloud formation, this may open the possibility of applying renormalization group machinery to this problem to better connect the detailed numerical simulations to the more understandable and useful simplistic models [13].

- [1] N. G. Loeb, B. A. Wielicki, D. R. Doelling, G. L. Smith, D. F. Keyes, S. Kato, N. Manalo-Smith, and T. Wong, *Journal of Climate* **22**, 748 (2009), ISSN 0894-8755, URL <http://journals.ametsoc.org/doi/full/10.1175/2008JCLI2637.1>.
- [2] K. E. Trenberth, J. T. Fasullo, and J. Kiehl, *Bulletin of the American Meteorological Society* **90**, 311 (2009), ISSN 0003-0007, URL <http://journals.ametsoc.org/doi/abs/10.1175/2008BAMS2634.1>.
- [3] T. Wong, T. Marvel, S. Lee, and V. Hopson, *Earth's Energy Budget Poster : Home* (2016), URL https://science-edu.larc.nasa.gov/energy_budget/.
- [4] S. Bony and J.-L. Dufresne, *Geophysical Research Letters* **32**, L20806 (2005), ISSN 1944-8007, URL <http://onlinelibrary.wiley.com/doi/10.1029/2005GL023851/abstract>.
- [5] I. Koren and G. Feingold, *Proceedings of the National Academy of Sciences* **108**, 12227 (2011), ISSN 0027-8424, 1091-6490, URL <http://www.pnas.org/content/108/30/12227>.
- [6] K. Peters, C. Jakob, L. Davies, B. Khouider, and A. J. Majda, *Journal of the Atmospheric Sciences* **70**, 3556 (2013), ISSN 0022-4928, URL <http://journals.ametsoc.org.proxy2.library.illinois.edu/doi/abs/10.1175/JAS-D-13-031.1>.
- [7] O. Peters and J. D. Neelin, *Nature Physics* **2**, 393 (2006), ISSN 1745-2473, URL <http://www.nature.com/nphys/journal/v2/n6/abs/nphys314.html>.
- [8] S. N. Stechmann and S. Hottovy, *Geophysical Research Letters* **43**, 2016GL069396 (2016), ISSN 1944-8007, URL <http://onlinelibrary.wiley.com/doi/10.1002/2016GL069396/abstract>.
- [9] A. Arakawa and W. H. Schubert, *Journal of the Atmospheric Sciences* **31**, 674 (1974), ISSN 0022-4928, URL <http://journals.ametsoc.org/doi/abs/10.1175/1520-0469%281974%29031%3C0674%3AIOACCE%3E2.0.CO%3B2>.
- [10] G. Feingold and S. M. Kreidenweis, *Journal of Geophysical Research: Atmospheres* **107**, 4687 (2002), ISSN 2156-2202, URL <http://onlinelibrary.wiley.com.proxy2.library.illinois.edu/doi/10.1029/2002JD002054/abstract>.
- [11] A. J. Lotka, *The Journal of Physical Chemistry* **14**, 271 (1909), ISSN 0092-7325, URL <http://dx.doi.org/10.1021/j150111a004>.
- [12] Volterra, V, *Mathematical biology: An introduction* **2**, 31 (1926).
- [13] J. Wettlaufer, *Physical Review Letters* **116**, 150002 (2016), URL <https://link.aps.org/doi/10.1103/PhysRevLett.116.150002>.